Effect of Weir Face Angles on Circular-Crested Weir Flow

Lukas Schmocker[1]; Berglind R. Halldórsdóttir[2]; and Willi H. Hager, F.ASCE[3]

Abstract: The standard circular-crested weir is often found in engineering applications and is used as a discharge measurement device or as an overflow structure. This research determines the discharge coefficients for ten circular-crested weir configurations with various combinations of up- and downstream angles. Two different weir heights and four different overflow depths are considered for each weir shape. For free overflow, the discharge coefficient is determined experimentally by using the total head of the approach flow. The results indicate that the upstream weir face angle has only a small effect on the discharge coefficient. In contrast, increasing the downstream weir face angle increases the discharge coefficient notably. A new formula for the discharge coefficient is presented, including both the up- and downstream weir face angles. Further, the hydraulic performance of the circular-crested weir, the resulting discharge reduction from tailwater submergence, and transition flow are discussed. **DOI: 10.1061/(ASCE)HY.1943-7900.0000346.**

CE Database subject headings: Weirs; Water discharge; Coefficients; Hydraulic models; Submerging.

Author keywords: Circular-crested weir; Discharge coefficient; Hydraulic modeling; Weir face angle; Submergence.

Introduction

Circular-crested weirs are primarily used for discharge measurement and as overflow structures. Their advantages include stable overflow condition, simplicity in design, and low cost. The weir is commonly designed with a circular crest of radius R, an upstream weir face perpendicular to the approach flow direction, and a downstream weir face angle of approximately 45°. In low-head dam applications, the downstream weir face angle is normally smaller. For free overflow, the discharge coefficient C_d and the overflow discharge Q are related as

$$Q = C_d b(2gH_o^3)^{1/2} \tag{1}$$

where b = overflow width; g = gravitational acceleration; and $H_o = h_o + Q^2/[2gb^2(h_o + w)^2]$ = approach flow (subscript o) energy head with h_o = overflow depth; and w = weir height. The effects of weir height w and weir geometry are contained in C_d. A proposal for C_d by Montes (1970) was adapted by Hager (1994b) as

$$C_d = \frac{2}{3\sqrt{3}}\left(1 + \frac{3\rho_k}{11 + \Omega\rho_k}\right) \tag{2}$$

with $\rho_k = H_o/R$ = relative crest curvature; and Ω = 4.5. An overview of empirical C_d formulas for these weirs is presented by Chanson and Montes (1998), but none of their reviewed formulas account for the effect of upstream (subscript o) and downstream (subscript d) weir face angles α_o and α_d. Note that the discharge coefficient of broad-crested weirs decreases as both α_o and α_d increase (Hager 1994a), a fact expected also for circular-crested weirs. The present research investigates this question.

Numerous studies have investigated the discharge over weirs. Bazin (1898) was the first to systematically investigate C_d for embankment weirs. His tests included trapezoidal weirs with α_o and $\alpha_d < 45°$, indicating a discharge reduction as the downstream weir face angle reduces. Three flow types were classified for embankment weirs: (1) free flow; (2) plunging nappe flow; and (3) submerged flow. Jaeger (1933a, b) used the Boussinesq equation to determine the discharge coefficient of circular-crested weirs. He stated that the discharge coefficient depends on the relative crest curvature R/H_o and the relative overflow depth h/H_o. Both Hégly (1939) and Jaeger (1940) presented formulas for C_d depending on H_o/R. The effect of small overflow depths on the free surface profile was studied by Bretschneider (1961) for weirs sloping 1:1 (V:H), 1:1.5, and 1:2.

Matthew (1963a, b) presented an equation for C_d including the effects of streamline curvature, viscosity, and surface tension, thereby accounting for scale effects in hydraulic modeling of overflow structures. The velocity distribution at the crest section and an equation for C_d were derived by Montes (1970). Lakshmana Rao and Jagannadha Rao (1973) and Lakshmana Rao (1975) investigated the coefficient of discharge for hydrofoil weirs, i.e., weirs whose top surface is curved similarly to a hydrofoil and taking into account the submergence limit. They found that C_d for hydrofoil weirs is higher than for the conventional rectangular broad-crested weir owing to streamline curvature effects. Bos (1976) presented a standard work on discharge measurement structures including circular-crested weirs with vertical upstream faces and downstream weir face angles of 45°. Depending on the tailwater depth, four different flow regimes downstream of the circular-crested weir were distinguished: (1) hydraulic jump, with toe located at or downstream of the weir; (2) plunging jet; (3) surface wave flow; and (4) surface jet flow. This classification was considered in the present study (Fig. 1). The effects of viscosity and surface tension on embankment weir flow were studied by Ranga Raju et al. (1990). They identified the characteristic parameter $\Phi = \mathsf{R}^{0.2}\mathsf{W}^{0.6}$ in which $\mathsf{R} = (gh_o^3)^{1/2}\nu^{-1}$ is the Reynolds number; $\mathsf{W} = \rho g h_o^2 \sigma^{-1}$ is the Weber number; υ is the fluid viscosity; ρ is fluid density; and

[1]Ph.D. Student, Laboratory of Hydraulics, Hydrology, and Glaciology VAW, Swiss Federal Institute of Technology ETH Zurich, CH-8092 Zurich, Switzerland (corresponding author). E-mail: schmocker@vaw.baug.ethz.ch

[2]M.Sc., ETH Civil Engineer, Basler and Hoffman Engineers, CH-8092 Zurich, Switzerland.

[3]Professor, Laboratory of Hydraulics, Hydrology, and Glaciology VAW, Swiss Federal Institute of Technology ETH Zurich, CH-8092 Zurich, Switzerland. E-mail: hager@vaw.baug.ethz.ch

Note. This manuscript was submitted on March 24, 2010; approved on October 10, 2010; published online on May 16, 2011. Discussion period open until November 1, 2011; separate discussions must be submitted for individual papers. This paper is part of the ***Journal of Hydraulic Engineering***, Vol. 137, No. 6, June 1, 2011. ©ASCE, ISSN 0733-9429/2011/6-637–643/$25.00.

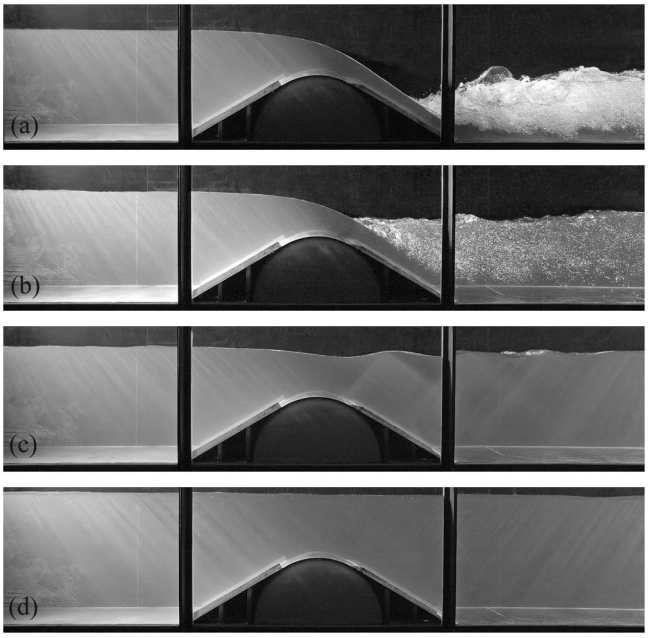

Fig. 1. Main flow patterns downstream of circular-crested weir: (a) hydraulic jump; (b) plunging jet; (c) surface wave flow; and (d) surface jet flow

σ is surface tension. For $\Phi > 10^3$, scale effects attributed to surface tension and viscosity are absent, almost independently of weir face angle, weir height, and discharge.

Ramamurthy and Vo (1993a) studied the effect of weir face angles on circular-crested weir flow. For a broad range of H_o/R, they tested angles of $\alpha_o = 60°$, 75°, and 90° and $\alpha_d = 45°$, 60°, and 75°, resulting in no effect of α_o on C_d for a fixed downstream angle. For a fixed α_o, they observed an increase of C_d as α_d increases. Ramamurthy and Vo (1993b) determined the weir discharge coefficient as a function of the total approach flow head and the crest radius by applying the theory of Dressler (1978). Chanson and Montes (1998) made tests on circular-crested weir overflow for various weir radii and weir heights, including an upstream ramp, stating that the upstream ramp had no effect on C_d but a major influence on the upstream flow conditions owing to streamline curvature. A general work on the hydraulics of embankment weirs was made by Fritz and Hager (1998), including the coefficient of discharge in terms of relative crest length for trapezoidal-crested weirs. Heidarpour et al. (2008) applied the potential flow theory to the circular-crested weir. They analyzed the crest velocity distribution, normalized crest pressure, and the pressure correction coefficient, and validated the resulting equations with laboratory data. A two-dimensional (2D) model for critical flow was developed by Castro-Orgaz (2008) and applied to the circular-crested weir. The discharge coefficient increased with the relative energy head including streamline curvature effects.

This study investigates the hydraulic features of the circular-crested weir of various up- and downstream weir face angles. The main parameters considered are: (1) free surface profile; (2) coefficient of discharge; (3) modular limit and transition range; and (4) discharge reduction under submerged flow. These results complete the hydraulic knowledge of circular-crested weirs. A new formula for the discharge coefficient is developed taking into account both weir face angles. The results apply to hydraulic structures in general, and to the 2D dike-breach problem in particular, because the circular-crested weir shape is similar to that of an embankment dike during erosion by overtopping (Schmocker and Hager 2009). Therefore, the present results apply also to the discharge features of these dike breaches.

Experimental Setup

Hydraulic Model

The experiments were conducted in a rectangular, horizontal channel at Laboratory of Hydraulics, Hydrology, and Glaciology VAW, of the Swiss Federal Institute of Technology ETH, Zurich, Switzerland. Its discharge capacity is 150 l/s, it is 0.50(±0.002) m wide, 0.70 m high, and 7.0 m long. A 250 mm conduit discharged the flow into the channel, whose uniformity was improved with a flow straightener rendering the approach flow free of surface waves and flow concentrations. The tailwater level was adjusted with a flap gate to the nearest mm. Discharges up to 60 l/s were determined with a standard V-notch weir (±0.1%) and up to 120 l/s with an electromagnetic flow meter (±0.5%). The axial free surface profile was taken with a point gauge of ±0.2 mm reading accuracy. Because of minor surface waves and tailwater turbulence, the observational accuracy was only ±5 mm in the tailwater.

Fig. 2 shows the test setup for both free and submerged overflow conditions in which h is flow depth, the weir face angles are α_o and α_d, x is the stream-wise coordinate measured from the weir crest, h_d is downstream depth, and h_t is the tailwater (subscript t) depth measured positively up from the weir crest. Circular-crested weir models were placed 3.5 m from the channel inlet. Two radii, $R = 0.15$ m and $R = 0.30$ m, were used, and both α_o and α_d were 20°, 30°, 45°, and 90°, resulting in a total of 20 weir models

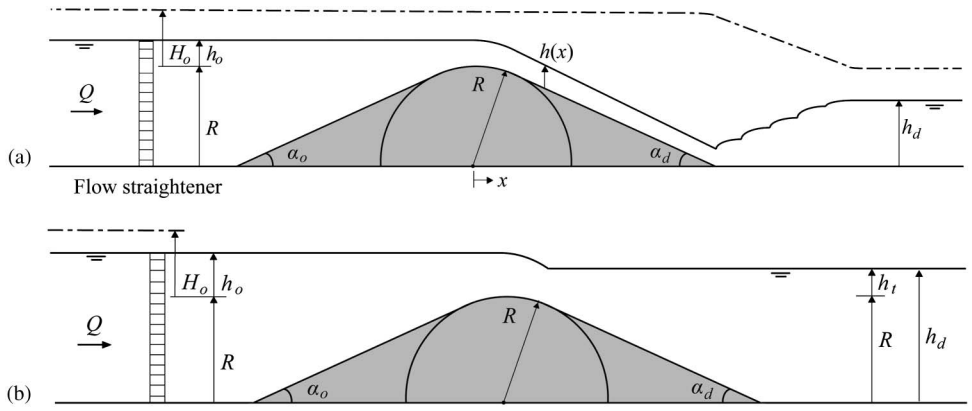

Fig. 2. Definition of flow geometry for (a) free; and (b) submerged overflow

J. Hydraul. Eng. 2011.137:637-643.

Table 1. Test Program, Weir Profiles Relating to Free Overflow Conditions

	$R = 0.3$ m (gray symbols)		$R = 0.15$ m (black symbols)		Weir face angles	
Symbol	Series	h_o (m)	Series	h_o (m)	α_o[°]	α_d[°]
○	01	0.05	11	0.075	30	30
		0.10		0.10		
		0.15		0.15		
		0.20		0.20		
□	02	0.05	12	0.075	90	30
		0.10		0.10		
		0.15		0.15		
		0.20		0.20		
◊	03	0.05	13	0.075	20	30
		0.10		0.10		
		0.15		0.15		
		0.20		0.20		
×	04	0.05	14	0.075	20	90
		0.10		0.10		
		0.15		0.15		
		0.20		0.20		
+	05	0.05	15	0.075	90	90
		0.10		0.10		
		0.15		0.15		
		0.20		0.20		
△	06	0.05	16	0.075	30	90
		0.10		0.10		
		0.15		0.15		
		0.20		0.20		
◺	07	0.05	17	0.075	20	20
		0.10		0.10		
		0.15		0.15		
		0.20		0.20		
⊞	08	0.05	18	0.075	90	20
		0.10		0.10		
		0.15		0.15		
		0.20		0.20		
⊠	09	0.05	19	0.075	90	45
		0.10		0.10		
		0.15		0.15		
		0.20		0.20		
▽	10	0.05	20	0.075	45	90
		0.10		0.10		
		0.15		0.15		
		0.20		0.20		

(Table 1). For each model, four overflow depths were tested, specifically $h_o = 0.05$, 0.10, 0.15, and 0.20 m for $R = 0.30$ m; and $h_o = 0.075$, 0.10, 0.15, and 0.20 m for $R = 0.15$ m.

Test Procedure

An identical test procedure was applied to all tests. First, the weir overflow depth was set. The hydraulic jump was then positioned at the downstream weir toe [Fig. 2(a)], and the discharge was determined. The free surface profile was measured along the channel axis. The point gauge was then placed 1 mm above the approach-flow water surface. The downstream flow depth was increased until the previously mentioned point gauge elevation was reached to determine the modular limit. The downstream water depth was further increased until the transition from the plunging jet to the surface wave regime occurred to determine the transition ranges. Again, both the up- and downstream water depths were measured. The overflow discharge was determined for various submergence ratios to account for the discharge reduction attributed to tailwater increase.

Observations and Results

Free Surface Profiles

Fig. 3(a) shows typical free surface profiles for Test 7. Note that the y-axis is stretched to allow for a better differentiation of the four profiles. The flow upstream of the weir is subcritical. Transitional flow occurs on the weir crest and the flow along the downstream weir face is supercritical. The critical (subscript c) flow depth $h_c = [Q^2/(gb^2)]^{1/3}$ is approximately located at the crest section.

J. Hydraul. Eng. 2011.137:637-643.

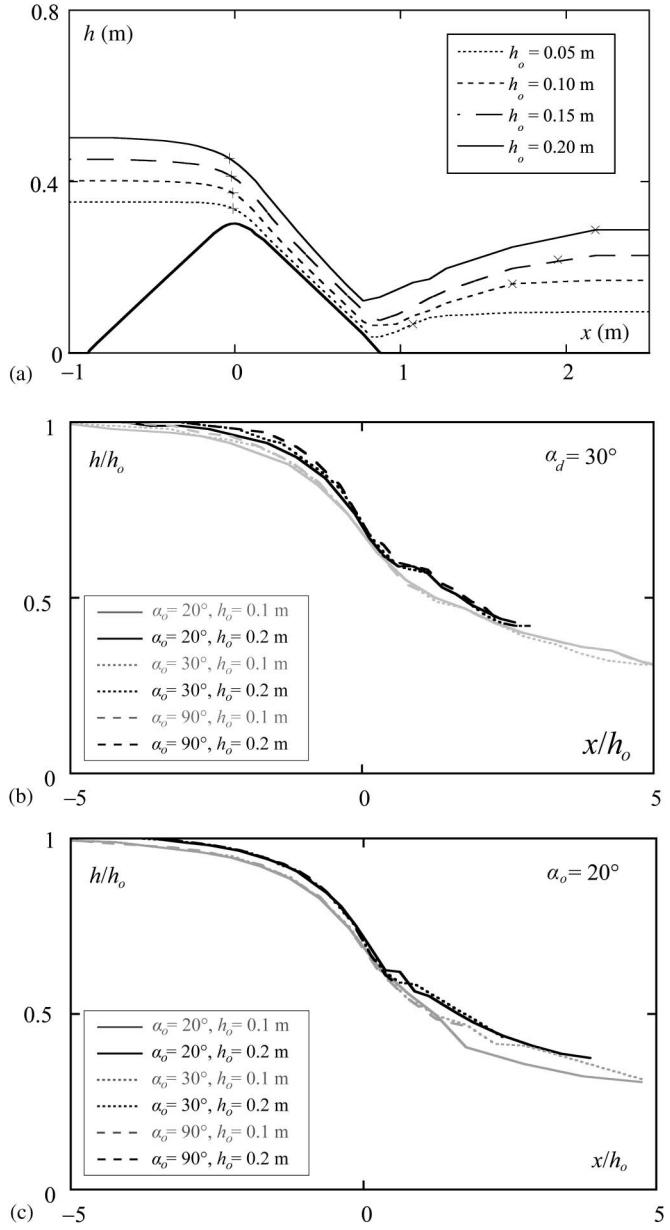

Fig. 3. Free surface profiles (a) $h(x)$ for Test 7 with (+) critical flow depth, (×) end of roller, and normalized free surface profiles $h/h_o[x/h_o]$ for (b) $\alpha_d = 30°$, $R = 0.30$ m, and various α_o; and (c) $\alpha_o = 20°$, $R = 0.30$ m, and various α_d for $h_o = 0.10$ m (gray) and $h_o = 0.20$ m (black)

The roller (subscript r) length L_r is approximately equal to that of the classical hydraulic jump (Hager 1992). Fig. 3(b) compares the dimensionless free surface profiles $h/h_o[x/h_o]$ for various values of α_o and $\alpha_d = 30°$, $R = 0.30$ m. The surface profiles almost collapse for two approach flow depths and all tested α_o. Note that the latter has practically no effect on the free surface profile as stated previously. Fig. 3(c) compares $h/h_o[x/h_o]$ for various values of α_d and $\alpha_o = 20°$, $R = 0.30$ m. Given the identical upstream weir face angle, the surface profiles again almost collapse at the inflow section. Differences occur for $x/h_o > 1$ as the downstream weir face angle affects the hydraulic jump flow profile.

Discharge Coefficient

For each overflow depth, the discharge coefficient was determined with Eq. (1) by using the measured discharge Q. The derived data $C_d(\rho_k)$ and Eq. (2) are shown for $\alpha_d = 90°$ and $\alpha_o = 20°$, 30°, 45°, and 90° in Fig. 4(a), whereas Fig. 4(b) relates to $\alpha_o = 90°$ and $\alpha_d = 20°$, 30°, 45°, and 90°. In general, the measured data are lower than Eq. (2) because the weir face angle effect was neglected. Note that C_d for the circular-crested weir with up- and downstream weir face angles is lower than that of the standard circular-crested weir. The data indicate that for fixed values of ρ_k and α_d, C_d barely changes with α_o [Fig. 4(a)] and is in agreement with Ramamurthy and Vo (1993a). The data for $\alpha_o = \alpha_d = 90°$ nearly collapse with Eq. (2). The data for $\alpha_d = 20°$ and $\alpha_d = 30°$ under variable α_o indicate similar results.

The data for fixed ρ_k and α_o under variable α_d indicate that C_d increases with α_d [Fig. 4(b)]. This effect becomes more apparent as ρ_k increases. The C_d coefficient is smallest for $\alpha_d = 20°$. A larger downstream weir face angle increases the discharge coefficient for a fixed overflow depth. Compared with α_o, the effect of α_d on the discharge is larger. Again, the data for $\alpha_o = \alpha_d = 90°$ nearly collapse with Eq. (2).

To account for the weir face angles, the weir crest effect was generalized to

$$\rho_k' = \frac{H_o}{R}\left(\frac{\alpha_o + 2\alpha_d}{270}\right)^{\frac{1}{3}} \tag{3}$$

where H_o/R = weir crest curvature effect and $[(\alpha_o + 2\alpha_d)/270]^{1/3}$ = weir face angle effect. As the effect of α_d is dominant, it is multiplied by 2, resulting, thereby, in the best data fit. For the standard circular-crested weir with $\alpha_o = \alpha_d = 90°$ results $[(\alpha_o + 2\alpha_d)/270]^{1/3} = 1$, and $\rho_k' = \rho_k = H_o/R$. Eq. (3) is limited to the weir profiles of Table 1. The discharge coefficient may then be expressed according to Hager (1994b) by using ρ_k' instead of ρ_k and $\Omega = 4.5$ as

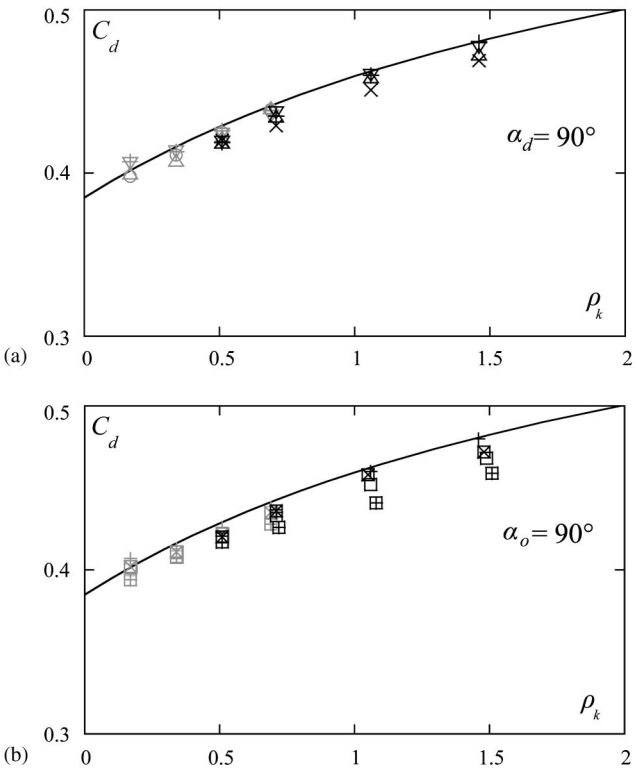

Fig. 4. Measured discharge coefficient $C_d(\rho_k)$ for (a) $\alpha_d = 90°$ and $\alpha_o = 20°$, 30°, 45°, and 90°; (b) $\alpha_o = 90°$ and $\alpha_d = 20°$, 30°, 45°, and 90° with (−) Eq. (2); symbols in Table 1

J. Hydraul. Eng. 2011.137:637-643.

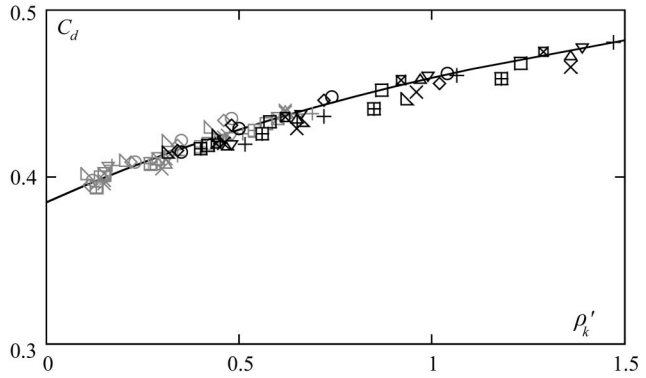

Fig. 5. Comparison of measured discharge coefficients $C_d(\rho_k\prime)$ with (−) Eq. (4); symbols in Table 1

$$C_d = \frac{2}{3\sqrt{3}}\left(1 + \frac{3\rho_k'}{11 + \Omega\rho_k'}\right) \tag{4}$$

Fig. 5 compares $C_d(\rho_k\prime)$ for all test data with Eq. (4) with a coefficient of determination of $r^2 = 0.92$. Accounting for the weir face angle ratio increases the data fit significantly compared with Fig. 4. Therefore, Eq. (4) can determine C_d of circular-crested weirs of arbitrary up- and downstream weir face angles if $0.1 \le \rho_k' \le 1.46$ with an accuracy of approximately ±2.5%. Keep in mind the limitation of the present study regarding the comparatively high overflow depth compared with the weir height. Further, no weir face angles between $45° \le \alpha \le 90°$ were investigated.

Comparison of Results

Ramamurthy and Vo (1993a) investigated the discharge coefficient for $\alpha_o = 90°$, 75°, and 60°; $\alpha_d = 75°$, 60°, 45°; and $0 \le H/R \le 25$. A maximum C_d was stated for $H/R = 5.5$ followed by a reduction of C_d for $H_o/R > 5.5$. Fig. 6 compares their data $C_d(\rho_k\prime)$ with Eq. (4) for $0 \le \rho_k\prime \le 6$. For $\rho_k\prime < 1$, Eq. (4) overestimates C_d, whereas Eq. (4) underestimates C_d for $\rho_k\prime > 1$. Compared with Ramamurthy and Vo (1993a), the dimensionless weir height w/H_o is comparatively low ($w/R = 1$) in the present study. Therefore, the weir height may have an effect on C_d. Ramamurthy and Vo (1993a) used weir model radii of $0.0095 \text{ m} \le R \le 0.1516$ m with $w/H_o \ge 3$. Their data indicate that C_d for $\rho_k' \to 0$ is below the theoretical value of $2/(3{\cdot}3^{0.5})$. This points at a scale effect primarily because of viscosity and partially because of surface tension owing to extremely small overflow depths. In the present study, scale effects were observed for $h_o < 0.05$ m, resulting in a reduction of the discharge coefficient.

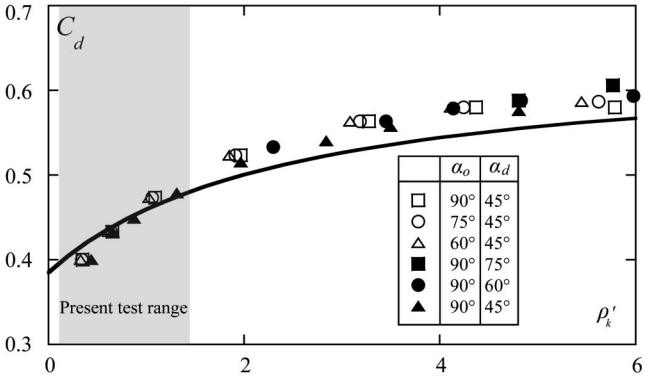

Fig. 6. Comparison of discharge coefficients $C_d(\rho_k\prime)$ of Ramamurthy and Vo (1993a) with (−) Eq. (4)

Modular Limit

The modular limit (subscript L) separates free from submerged overflow. The submergence degree can be described as $y_t = h_t/h_o$. For free flow, the discharge is independent of y_t. Submerged overflow is characterized by an increase of +1 mm overflow depth h_o because of tailwater elevation. Fig. 7(a) shows the modular limit ratio $y_L = h_{tL}/h_o$ versus ρ_k'. It may be expressed with $r^2 = 0.88$ as

$$y_L = 0.57 + 0.12\rho_k' \tag{5}$$

Accordingly, the modular limit increases linearly with ρ_k'. The scatter of data is considerable, yet without definite effects of H_o/R and both α_o and α_d. For $\rho_k' < 0.5$, small effects of scale may contribute to the data scatter despite $H_o > 0.05$ m. Therefore, the modular limit ratio is more or less independent from both weir face angles. Circular-crested weirs are less prone to submergence than sharp-crested weirs. Free flow is generated for circular-crested weirs between 50 and 80% of submergence, which is similar to trapezoidal-crested weirs (Fritz and Hager 1998).

Transition Submergence

At a certain tailwater depth h_{tT}, increasing the tailwater level results in a transition (subscript T) from plunging jet to surface wave flow. Then, by reducing the tailwater level, the transition from surface wave to plunging jet flow occurs at another tailwater depth. Fig. 7(b) shows the submergence ratio $y_T = h_{tT}/h_o$ as a function of ρ_k' under increasing tailwater level. The best-fit equation is ($r^2 = 0.55$)

$$y_T = 0.97 + 0.039 \cdot \ln(\rho_k') \tag{6}$$

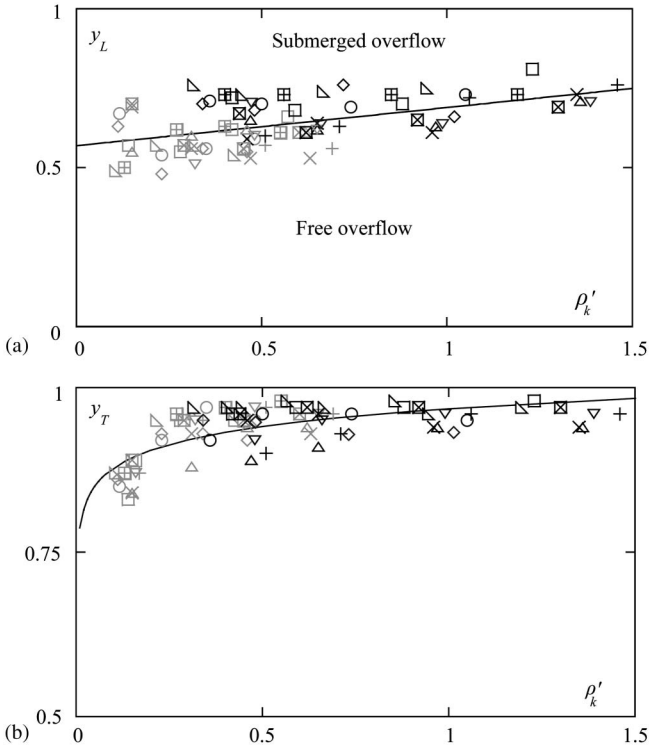

Fig. 7. (a) modular limit $y_L(\rho_k\prime)$ with (−) Eq. (5); and (b) transition submergence $y_T(\rho_k\prime)$ with (−) Eq. (6); symbols in Table 1

J. Hydraul. Eng. 2011.137:637-643.

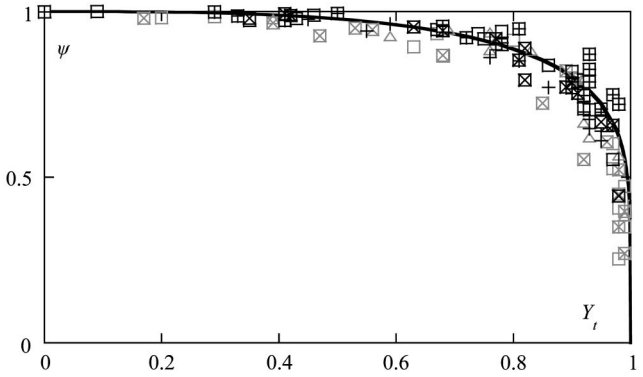

Fig. 8. Discharge reduction factor ψ as a function of relative submergence Y_t; symbols in Table 1

Therefore, a high submergence ratio is reached compared with trapezoidal-crested weirs, with y_T increasing with ρ'_k. The transition submergence has a lower value of $y_T = 0.84$ for $\rho'_k = 0.1$, increases to $y_T = 0.95$ for $\rho'_k = 1.45$, and then remains almost constant for $\rho'_k \geq 0.75$. Plunging flow results for $y_T < 0.84$, whereas surface wave flow occurs if $y_T > 0.95$. Between $0.84 < y_T < 0.95$, both flow types may occur. No effect of weir face angle on y_T was found.

Discharge Reduction by Submergence

The discharge Q_s of submerged (subscript s) weir flow is equal or smaller than the discharge Q for free overflow. The discharge reduction factor $\psi = Q_s/Q$ depends exclusively on the submergence ratio $y_t = h_t/h_o$ because all other parameters are contained in Q. The factor ψ varies between $\psi = 0$ for $y_t(h_t = h_o) = 1$ and $\psi = 1$ for $y_t(h_t = h_{tL}) = y_L$. To generalize results, the relative submergence $Y_t = (y_t - y_L)/(1 - y_L)$ with $0 < Y_t < 1$ according to Fritz and Hager (1998) was used. Fig. 8 shows $\psi(Y_t)$ with $r^2 = 0.40$ for selected tests as

$$\psi = (1 - Y_t^3)^{1/6} \tag{7}$$

No decisive effect of either $H_o/R, \alpha_o$ or α_d is visible because all data collapse more or less on a single curve. Note that the discharge reduction for a certain value of Y_t is slightly smaller for flat than for steep downstream weir face angles.

Conclusions

The discharge coefficient for circular-crested weirs of various up- and downstream weir face angles was experimentally investigated by using fixed weir profiles. The results indicate effects of the relative weir radius and the downstream weir face angle. A generalized equation for the discharge coefficient of circular-crested weirs including up- and downstream weir face angles is presented for weirs with a relatively modest crest curvature. Both the modular limit ratio and the transition submergence are more or less independent from both weir face angles, and circular-crested weirs are less prone to submergence effects than sharp-crested weirs. Furthermore, the discharge reduction by submergence is nearly independent of the weir face angles. A comparison with existing data indicates deviations primarily attributable to different test setup and scale effects.

Acknowledgments

The first author was supported by the Swiss National Science Foundation, Grant No. 200020-116680.

Notation

The following symbols are used in this paper:

b = overflow width;
C_d = discharge coefficient;
g = gravitational acceleration;
H = energy head;
h = flow depth;
Q = discharge;
R = Reynolds number;
R = crest radius;
r = coefficient of determination;
W = Weber number;
w = weir height;
x = streamwise coordinate;
Y = relative submergence;
y = degree of submergence;
α = weir face angle;
ρ = density;
ρ_k = relative crest curvature;
ρ'_k = dimensionless parameter;
σ = surface tension;
ν = kinematic viscosity;
Φ = scale parameter;
ψ = submergence factor; and
Ω = constant.

Subscripts

c = critical;
d = downstream;
L = modular limit;
r = roller;
T = transition;
t = tailwater; and
o = upstream.

References

Bazin, H. (1898). "Expériences nouvelles sur l'écoulement en déversoir [New experiments on weir discharge]." *Ann. Ponts Chaussées*, 68(2), 151–265 [in French].

Bos, M. G. (1976). "Discharge measurement structures." *Rapport 4*. Laboratorium voor Hydraulica an Afvoerhydrologie, Landbouwhogeschool, Wageningen, Netherlands.

Bretschneider, H. (1961). "Abflussvorgänge bei wehren mit breiter krone [Hydraulics of broad-crested embankment weirs]." *Mitteilung 53*. Institut für Wasserbau und Wasserwirtschaft, Technische Universität, Berlin [in German].

Castro-Orgaz, O. (2008). "Curvilinear flow over round-crested weirs." *J. Hydraul. Res.*, 46(4), 543–547.

Chanson, H., and Montes, J. S. (1998). "Overflow characteristics of circular crested weirs: Effects of inflow conditions." *J. Irrig. Drain Eng.*, 124(3), 152–162.

Dressler, R. F. (1978). "New nonlinear shallow flow equations with curvature." *J. Hydraul. Res.*, 16(3), 205–222.

Fritz, H. M., and Hager, W. H. (1998). "Hydraulics of embankment weirs." *J. Hydraul. Eng.*, 124(9), 963–971.

Hager, W. H. (1992). *Energy dissipators and hydraulics jumps*, Kluwer, Dordrecht, Netherlands.

Hager, W. H. (1994a). "Dammüberfälle [Dam Overflows]." *Wasser und Boden*, 45(2), 33–36 [in German].

Hager, W. H. (1994b). "Discussion of 'Momentum model for flow past weir', by A. S. Ramamurthy, N.-D. Vo., and G.Vera." *J. Irrig. Drain Eng.*, 120(3), 684–685.

Hégly, V. M. (1939). "Expériences sur l'écoulement de l'eau au-dessus et en dessous des barrages cylindriques [Discharge over and below cylindric weirs]." *Ann. Ponts Chaussées*, 109(9), 235–281 [in French].
Heidarpour, M., Habili, J. M., and Haghiabi, A. H. (2008). "Application of potential flow to circular-crested weir." *J. Hydraul. Res.*, 46(5), 699–702.
Jaeger, C. (1933a). "Notes sur le calcul des déversoirs et seuils [Discharge calculations for weirs and sills]." *Bull. Tech. Suisse Romande*, 59(13), 153–156 [in French].
Jaeger, C. (1933b). "Notes sur le calcul des déversoirs et seuils [Discharge calculations for weirs and sills]." *Bull. Tech. Suisse Romande*, 59(14), 166–169 [in French].
Jaeger, C. (1940). "Erweiterung der Boussinesq'schen Theorie des abflusses in offenen gerinnen: Abflüsse über abgerundete wehre [Extension of the Boussinesq Theory for open channel flow: Flow over round-crested weirs]." *Wasserkraft und Wasserwirtschaft*, 35(4), 83–86 [in German].
Lakshmana Rao, N. S. (1975). "Theory of weirs." *Advances in hydroscience*, V. T. Chow, Ed., Academics Press, New York, 10, 309–406.
Lakshmana Rao, N. S., and Jagannadha Rao, M. V. (1973). "Characteristics of hydrofoil weirs." *J. Hydraul. Div.*, 99(HY2), 259–283.
Matthew, G. D. (1963a). "On the influence of curvature, surface tension and viscosity on flow over round crested weirs." *ICE Proc.*, 25(4), 511–524.
Matthew, G. D. (1963b). "On the influence of curvature, surface tension and viscosity on flow over round crested weirs." *ICE Proc.*, 28(4), 557–569.
Montes, J. S. (1970). "Flow over round crested weirs." *L'Energia Elettrica*, 47(3), 155–164.
Ramamurthy, A. S., and Vo, N.-D. (1993a). "Characteristics of circular crested weir." *J. Hydraul. Eng.*, 119(9), 1055–1062.
Ramamurthy, A. S., and Vo, N.-D. (1993b). "Application of Dressler theory to weir flow." *J. Appl. Mech.*, 60(1), 163–166.
Ranga Raju, K. G., Srivastava, R., and Porey, P. D. (1990). "Scale effects in modelling flows over broad-crested weirs." *Irrig. Power India*, 47(3), 101–106.
Schmocker, L., and Hager, W. H. (2009). "Modelling dike breaching due to overtopping." *J. Hydraul. Res.*, 47(5), 585–597.

J. Hydraul. Eng. 2011.137:637-643.